View Article Online
DOI: 10.1039/C7EE03155F

Issue 3, 2018

Journal Name

ARTICLE

Revisiting lifetimes from transient electrical characterization of thin film solar cells; a capacitive concern evaluated for silicon, organic and perovskite devices†

Received 00th January 20xx,
Accepted 00th January 20xx

DOI: 10.1039/x0xx00000x

www.rsc.org/

D. Kiermasch,[a] A. Baumann,[b] M. Fischer[a], V. Dyakonov[a,b] and K. Tvingstedt*[a]

The lifetime of photogenerated charge carriers is one of the most important parameters in solar cells, as it rules the recombination rate that defines the open circuit voltage and the required minimum extraction time. It is therefore also one of the most discussed factors in all photovoltaic research fields. Lifetime evaluation of solar cells is frequently conducted via both optical and electrical means with the purpose of obtaining a deeper understanding of the dominant performance limiting recombination mechanisms. In many earlier recombination designations, performed via transient electrical means in novel thin film solar cells, the lifetime has been observed to be a decaying exponential function of the open circuit voltage. In this work we re-evaluate these previously assigned lifetimes as often being severely influenced by capacitive decay rates of spatially separated charge carriers. These "lifetimes" have thus very little in common with lifetimes relevant under steady state operational conditions of the solar cell. We show that the problem of lifetime determination via electrical means arises from that the relaxation of such charges, being associated with quasi-static capacitances of geometric type or from space-charge regions in the device, is also a decaying exponential function of the instantaneous open circuit voltage. This misconception hence also explains the often observed large discrepancy between optically and electrically determined lifetimes. We finally provide a simple expression outlining under what conditions relevant bulk recombination lifetimes are electrically accessible in thin film solar cells.

[a] Experimental Physics VI, Julius Maximillian University of Würzburg, 97074 Würzburg, Germany
[b] Bavarian Center for Applied Energy Research 97074 Würzburg, Germany.
*Corresponding author: Kristofer Tvingstedt. E-mail: ktvingstedt@physik.uni-wuerzburg.de
†Electronic Supplementary Information (ESI) available: [Experimental details of manufacturing and measurement methodology]. See DOI: 10.1039/x0xx00000x

View Article Online
DOI: 10.1039/C7EE03155F

Introduction and background

The build-up and disappearance of charge carrier densities in solar cells involve a variety of processes including absorption and charge carrier generation, separation, transport via drift and diffusion, recombination in the bulk, via traps, at the surfaces or from the electrodes themselves. All these processes occur on time scale ranging from sub-picoseconds[1] to in some cases several seconds or even hours.[2] Effectively designing photovoltaic components for optimizing power conversion efficiency always relies on maximizing the carrier generation and transport processes and simultaneously minimizing the recombination processes towards the radiative limit of the material.[3] Identifying the recombination mechanism and its corresponding rate is therefore one of the most fundamental subject for any photovoltaic researcher, independent of material and technology. Both optical and electrical transient measurements are therefore frequently employed with the purpose to approach this. Contactless optical methods such as transient absorption, transient photoluminescence, and transient photo-conductance measurements all provide information related to the overall disappearance rate of excited states or charge carriers in the active material. Direct electrical measurements of contacted photovoltaic materials probe instead the disappearance rate of the electrochemical potential of the excess carrier densities. In semiconductor terminology, this parameter is referred to as the splitting of the quasi Fermi levels for electrons and holes, and is furthermore equivalent with the term often encountered within impedance analysis as the diffusion or chemical capacitance. Monitoring the rate at which this property decays provides accordingly the sought-after information of how the associated excess charge carriers disappear in a solar cell. In the time-domain, the most common methods employed are based on measuring the decay of the open circuit voltage, either by the full signal open circuit voltage decay (OCVD) method[4-7] or by the small perturbation method of transient photovoltage (TPV)[8-10]. In the corresponding frequency-domain, the rates are monitored by impedance spectroscopy[11-13] or intensity modulated voltage or current spectroscopy (IMVS/IMPS). All rate determination methods need a complementary measurement of the relationship between carrier density and voltage; for the time-domain methods this is provided by either combining transient photocurrent (TPC) with TPV and referred to as differential charging[9], or alternatively by the full signal charge extraction method (CE).[10, 14] The frequency-domain-methods rely instead commonly on the integral of various forms of differential capacitance-voltage measurements (C-V).[12, 13] Both the time-domain and frequency-domain methods are therefore in principle able to determine the rate/lifetime as a function of excess carrier density and have been regularly conducted for many different photovoltaic technologies during the last decades. However, there is caveat with these methods originating from that they were initially developed for thicker indirect bandgap germanium or silicon solar cells. Devices comprising these inorganic crystalline materials are very different compared to many novel thin film solar cells mostly in terms of their carrier lifetimes, but also in their capacitances and band gaps. Thin film solar cells are necessarily relying on materials with higher absorption coefficients, such as those based on dye sensitized solar cells (DSSC) organics (OPV), lead sulfide quantum dots (PbS), as well as metal halide perovskites, all with active layer film thickness in the range of 20-500nm. A high absorption coefficient is from reasons of reciprocity relations[3] always linked with a high radiative rate constant and therefore an inherent very short charge carrier lifetime. The high absorption coefficient allows a smaller thickness that however leads to devices with larger capacitance values. Another parameter related to the bandgap of the semiconductor material is the dark saturation current density (J_0) that rules the overall recombination dynamics at thermal equilibrium conditions. The value of this parameter is of fundamental importance for electrical lifetime determination methods as it ultimately rules the capacitance discharging rate of diodes,[2, 15] which will also be the main emphasis of this work. The electrical characterization methods employed to determine recombination dynamics in terms of charge carrier lifetimes, are therefore not always easily transferable to many new generation thin film photovoltaic devices, often with direct band gap and high absorption coefficients. A careful consideration of what is actually being measured is therefore imperative, and also the incentive of this contribution.

Carrier lifetime determination via electrical means was first proposed and conducted via voltage decay measurements by Lederhandler and Giacoletto for germanium already in 1955[4]. When similar electrical transient methods were introduced by Duffy[16] (full signal), O´Reagan[17] (small perturbation) for DSSC and later by Shuttle[8] for OPVs and Roiati[18] for perovskite solar cells, a strong nonlinear dependence of charge carrier lifetimes on voltage was observed. This dependence has later been reproduced for a plethora of other DSSC, PbS and organic cells and more recently also observed for a majority of novel lead halide

View Article Online
DOI: 10.1039/C7EE03155F
Journal Name ARTICLE

perovskite solar cells.[19-26] The observed strong dependence on illumination intensities has justly been interpreted as that the dynamics cannot be described by a simple first order recombination process (where carrier lifetime should be constant over at least some range of excess carrier densities). The very long lifetimes, often several seconds[7] at lower voltages, seen in DSSC are generally attributed to a slow second order chemical reaction rate between electrons and ions present in the electrolyte. However, a quite identical dependence is also observed in most organic, PbS and perovskite based solar cells studied so far. In these solid state components, slow chemical reactions can by no means be used to generally explain the charge carrier kinetics. In analogy with the DSSC, a power law dependence of recombination rates with (bimolecular) second or higher order recombination kinetics in combination with assumptions of trapped charges in a broad density of states (DOS) has often been ascribed to account for both the strong dependency of voltage and the very slow rates. In this common picture, the long lifetimes originate from a nonlinear relationship between trapped and free charges, where shallow traps, not speeding up recombination as is generally the case for mid gap (deep) trap states, instead slow down the overall recombination rate. The trap distribution is often associated with an exponential tail distribution with a characteristic Urbach energy, which is also in principle accessible from the relationship between voltage and carrier density.[27-29]

Small perturbation lifetimes determined via electrical transients are for most of the mentioned photovoltaic technologies ranging typically from ~1 microsecond at sun intensities down to several milliseconds or seconds at reduced intensities. The empirical relationship observed implies that the charge carrier lifetime (τ) decays exponentially with increasing open circuit voltage according to:

$$\tau = \tau_0 e^{-\frac{qV_{OC}}{\upsilon kT}} \qquad [1]$$

where kT has its usual meaning and v is a fit factor accounting for the slope deviation in analogy with the ideality factor. In this expression, we remind that the prefactor τ_0 should correspond to the lifetime of equilibrium charge carrier densities (at zero voltage/dark conditions). In a majority of the earlier published works where eqn. 1 is implemented, we note that for higher bandgap materials the value of τ_0 takes extremely high values of up to several (thousands) seconds. The very long measured lifetimes of excess charge carriers (out of equilibrium/under illumination) are also quite peculiar. Often they are several decades longer than those determined via complementary optical measurements such as photoluminescence decay, terahertz spectroscopy or microwave conductivity measurement. For OPVs, where PL lifetimes of the charge transfer states lie in the range of 100 ps to 30 ns,[30-33] display instead electrically determined lifetimes ranging between a few microseconds at 1 sun and up to several hundred milliseconds at lower intensities. Similar lifetime discrepancies are now also often reported for perovskite solar cells. Both the optical and the electrical methods are claiming to probe charge carrier lifetimes relevant for steady state conditions, but obviously cannot both be correct when determined at equal carrier densities.

Apart from the huge discrepancies of reported lifetimes, added concern arises from the associated recombination orders, as is always accessible from the combined electrical transient measurements. Empirical recombination orders can be identified as the slope in a log-log plot of measured recombination rate vs. charge carrier density (or likewise as the inverse slope of lifetimes vs. carrier densities). Generally, first, second and third order recombination dynamics are well understood and associated with heavy doping or traps, band-to-band (generally assumed to be radiative) and Auger recombination, respectively. Auger recombination requires however extraordinary high charge carrier concentrations before it starts to rule the dynamics. Yet, in many earlier works, empirical reaction orders higher than two have often been reported at carrier densities not at all being particular high, and whose origin is for the most part not at all satisfactorily clarified. The higher orders reported have however by drift/diffusion simulation methods, performed by Kirchartz[29] and Deledalle[34, 35] for OPVs, instead been suggested to originate from a possible misinterpretation related to unknown spatial carrier density profiles with respect to the also unknown unintentional doping profiles, suggested to occur in many thin film solar cells. In this work, we provide unambiguous experimental evidence for that an analogous and quite simple explanation is responsible for both the slow "recombination rates" as well as the oddly high recombination orders sometimes encountered in thin film solar cells. Herein, we determine charge carrier lifetimes via both OCVD and TPV methods and show that the obtained lifetimes are in fact very often associated with a capacitive discharging rate. The objective of this work is therefore to experimentally clarify the general influence of such quasi-static capacitive effects on charge carrier lifetime determination by electrical time domain approaches.

View Article Online
DOI: 10.1039/C7EE03155F

Results and discussion

Devices

For sake of technological generality we herein experimentally evaluate four different solar cells with very diverse properties to highlight the overall message. The manufacturing of three of these are outlined in the supplementary information. As additional reference we evaluate an ideal monocrystalline (m-C) KG-5 filtered Si photodiode (S1787-04 Hamamatsu) as this device allows for an evident distinction between capacitive and bulk charge carrier densities and their corresponding lifetime, in line with that already demonstrated via frequency domain measurements[12] by Mora-Sero et. al. As clear counterexample we provide results from a high bandgap PCDTBT:PCBM thin OPV cell that is completely governed by geometric capacitive discharging. We show also the outcome of a planar methylammonium lead iodide (MAPI) perovskite solar cell, and a lower bandgap P3HT:PCBM OPV cell, which are most probably not ruled by a simple geometric capacitance, yet wherein true lifetime assignments are still as difficult.

To put the selected set of photovoltaic devices and their performance in relation to each other we first show their dark and illuminated I-V curves on lin.-log. axis in **Figure 1**. The device characteristic figures of merit for the four devices are also presented below in **Table 1**. The ideality factors of the cells range from exactly one for the Si photodiode to exactly two for the MAPI perovskite cell, with the two OPV cells ranging in between.

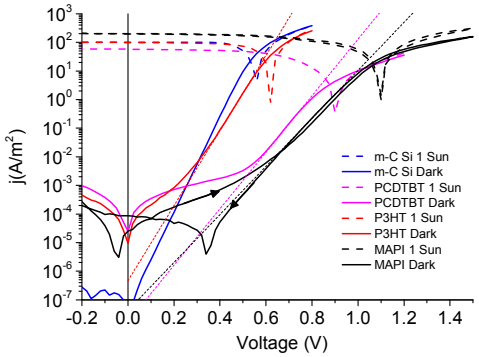

Figure 1. Dark and illuminated I-V characteristics of the four types of solar cells evaluated.

Carrier density determination and capacitance correction

We will first highlight that the density of excess charge carriers in the neutral bulk region is often difficult to determine correctly by electrical means such as charge extraction, differential charging and C-V in several types of thin film solar cells. What is actually often measured is partly remaining charge carriers stored in or at the respective electrodes of the device. The first raised concerns should therefore be evident when plotting electrically determined average carrier density vs. internal voltage, of which V_{OC} is generally the best representative.[36] Numerous publications do this, but often note merely a small increase of carrier density when the internal voltage is increased by several hundreds of millivolts. This is clearly in strong contrast to the expected strong exponential relationship between excess charge carrier densities and quasi-Fermi-level splitting (V_{OC}). Depending on doping concentrations and the distribution of trap densities in the intrinsic layer, the exponent should only be able to range between *kT/q* and *2kT/q* depending accordingly on whether the cell is operating in the low or high injection regime[37] (excess carriers being lower or higher than the doping/defect concentration). What are however often seen are values with slopes substantially lower than *2kT/q*. The reason is that one is often just not able to collect the total average excess minority carrier densities from the bulk but still mostly remaining spatially separated "capacitive" charge carriers. The uneven distribution of excess charge carriers under steady state open circuit conditions[34, 38] simply renders very different recombination rates at different positions within the device. The presence of such general capacitive contribution to the overall carrier density is nonetheless already well recognized in literature and also considered to be attended to. Two capacitive correction methods for carrier density determinations are mostly employed; the first is based on the assumption of a linear dielectric geometrical

Table 1.

	Ideality	J_0 [A/m^2]	J_{SC} [A/m^2]	V_{OC} [V]	FF	PCE [%]
m-C Si photodiode (KG-5)	1.0	5.2E-8	101	0.56	0.69	3.9
PCDTBT:PCBM60 (Thin)	1.7	1.7E-8	58	0.90	0.52	2.8
P3HT:PCBM60	1.28	4.64E-7	99	0.63	0.62	3.9
MAPI Perovskite	2.0	4.2E-8	198	1.10	0.56	12.2

View Article Online
DOI: 10.1039/C7EE03155F
Journal Name ARTICLE

capacitance ("charges on the plates") being identical in forward and reverse bias direction measurements. Accordingly, by measuring extracted charges from reverse biased solar cells in the dark one knows the capacitive correction needed also under forward illuminated bias. The second method, implemented when performing impedance measurements[13], is based on the assumption of different frequency response of different species in C-V sweeps. Capacitive charges at the electrodes are assumed to respond very fast, whereas excess minority bulk carriers in the neutral region are assumed to be much slower.[13] The sought-after bulk excess carrier density is then determined by evaluating the difference of a low and a high frequency C-V sweep. We here note that such corrections are extremely necessary but still insufficient to provide accurate estimates of average excess carrier concentrations in the bulk under reduced illumination intensities. Excess charge carriers in the bulk are expected to show an exponential relationship to internal voltage following the definition of their chemical potential in a Fermi-Dirac or Boltzmann distribution, whereas geometrical or space charge capacitive charge carriers show a much weaker (linear or power law) dependence. Subtracting such weak dependencies from an exponential relation at best gives improvement in accuracy of carrier concentration in a rather narrow voltage range but does not at all help at lower voltages. Accordingly, the charge carrier density plotted on a logarithmic scale vs. the internal voltage must provide a clear and distinguishable transition from the capacitive contribution in the low voltage region to a clear and strong exponential function[12, 13] at higher internal voltages. If such trends in the logarithmic Δn vs. V_{OC} plot cannot be identified at least at higher voltages, and values substantially larger than $2kT/q$ in the denominator are instead identified everywhere, it is probable that the device is not suited for electrical measurements with the aim of providing relevant information regarding steady state charge carrier lifetimes and recombination orders. Such prefactors to the thermal voltage (kT/q) in the denominator of the exponent have in recent literature[29] been assigned with the letter m and we use that here as well to distinguish it from the normal ideality factor. Independent of origin, the empirically determined relationship between excess carrier concentration and voltage usually follows:

$$\Delta n = n_0 e^{\frac{qV_{OC}}{mkT}} \qquad [2]$$

where n_0 should correspond to equilibrium carrier concentration. Earlier expressions[8] used constants that instead included also the thermal voltage (kT/q), but as temperature is a free accessible experimental parameter such approach must be considered inferior.

View Article Online
DOI: 10.1039/C7EE03155F

Figure 2 displays the total measured charge vs. voltage for the Si photodiode, the two organic solar cells and the perovskite cell, as obtained from both CE and C-V measurements. The raw data provided directly from CE measurements are represented by black dots and plotted vs. V_{OC}. The corrected charge (red dots) is determined by subtracting the charge obtained from reverse biased dark charge extraction. We emphasize to the reader that we have deliberately refrained from assigning charge carrier *density* on the y-axis, but instead speak only of total charge. The reason is related to the core of the manuscript concerning the differentiation between capacitive charge carriers and bulk charge carriers. The first are not true volume charges, but possibly better described as charges distributed over an area (surface charge density) and their unit may accordingly be different from the bulk charges which are indeed distributed in volume.

The Si cell (in panel A) easily allows for the clear identification of a strong exponential contribution from carriers in the bulk at voltages >450mV as well as of a clear depletion layer capacitive contribution at lower voltages (blue curve shows the charge associated with a Mott-Schottky fit). We also include (dashed magenta) the charge obtained from integrating a low frequency dark C-V sweep, evaluated in the parallel mode[39] vs. externally applied voltage ($V_{appl.}$), to ratify that the two methods are indeed measuring quite identical values, at least at lower voltages. Upon executing the C-V frequency difference correction we confirm that the result (green line) is very similar as obtained from the reverse bias charge extraction correction. The supplementary information provides a summary of the C-V sweeps for all four cells (**Figure S1**).

The raw extracted charge from the two organic cells does on the other hand not noticeably display the expected exponential region whereas the corrected charge shows a steeper, yet still not clearly exponential relation to internal voltage. For the P3HT cell (panel C) we have also included the measured extracted charge when the cell is placed in parallel with a 6.8 nF external

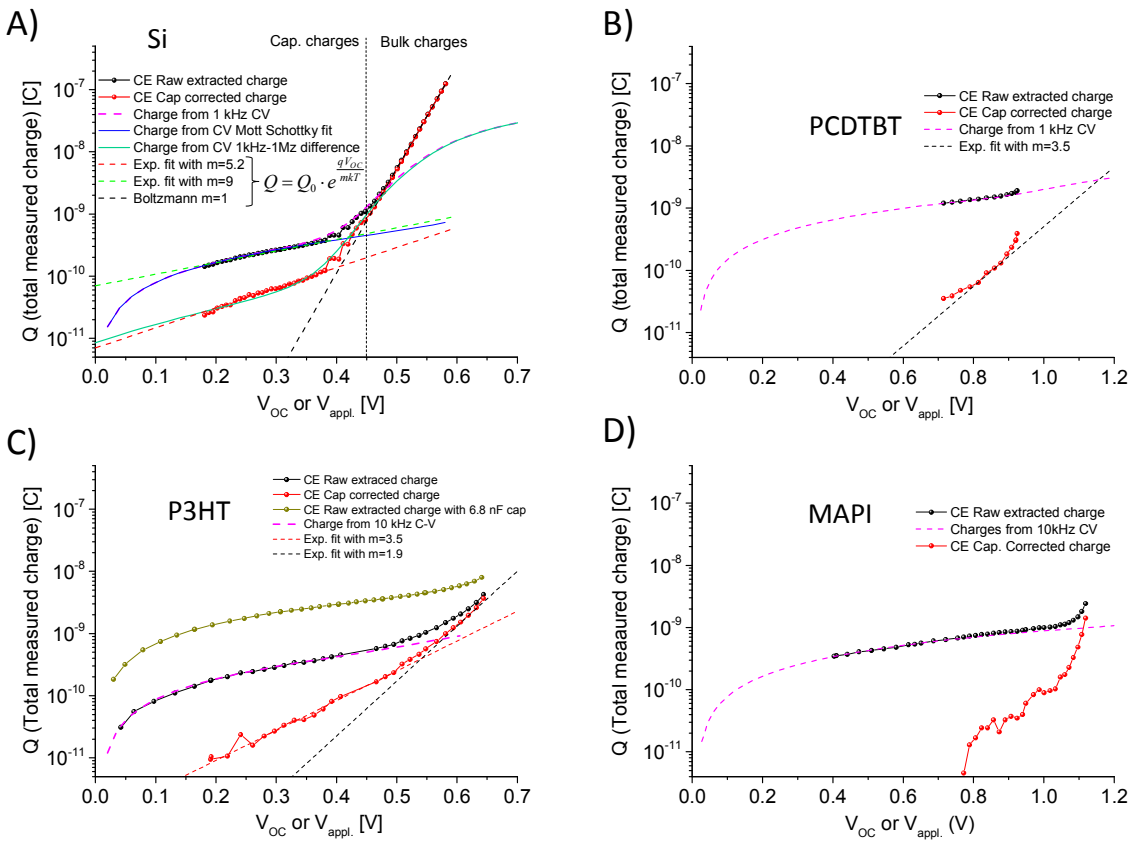

Figure 2. Measured charge from charge extraction (CE) vs. internal voltage (V_{oc}) and from capacitance-voltage (C-V) vs. externally applied voltage ($V_{appl.}$) for a Si photodiode (A) and the three thin film solar cells PCDTBT:$PC_{60}BM$ (B), P3HT:$PC_{60}BM$ (C) and MAPI (D). The charge from C-V is here not yet corrected for series resistance voltage drops. The P3HT:$PC_{60}BM$ panel (C) also include the CE data obtained from a cell in parallel with a 6.8 nF capacitor, to effectively demonstrate the capacitance contribution to charge extraction.

View Article Online
DOI: 10.1039/C7EE03155F
Journal Name ARTICLE

capacitor to demonstrate the overall impact of capacitive charge on these measurements. The perovskite cell does on the other hand appear to show a quite steep rise at the very highest voltages, all obtained from intensities exceeding 1 sun, pointing towards the possible onset of extraction of true bulk charges. At voltages lower than 1 V it is however fully ruled by capacitive charges. The integrated dark C-V measurements (corresponding to charge) does only show the exponential increase for the Si cell, but as C-V was measured via applied external voltage and here not corrected for series resistance, the deviations to the charge obtained from CE vs. V_{OC} are considerable (as expected) at higher voltages. It is however important to note that the three thin film devices do not even show a tendency of a steeper regime in the C-V measurements, clarifying that the overall capacitive contribution to total charge is indeed substantial. Capacitive correction methods are for these devices therefore extremely needed but unconditionally rendering rather large error margins in the obtained relation between corrected charge and V_{OC}. We also point out that subtracting charge associated with a depletion layer capacitance rather than a linear geometric capacitance renders quite different resulting slopes of the corrected data. Fitting the corrected charge with the exponential relation of eqn. 2 to determine the slopes (m-values) is still possible. Although decent exponential fits can be obtained even in the fully capacitive region for the Si cell, the resulting high m-values of 5 (corrected) or 9 (uncorrected) are not at all meaningful.[29] We remind that such high *m*-values around 5 are nonetheless very often observed in OPV, DSSC and perovskite literature. The slope of the relevant excess minority carriers in the bulk is however found only at voltages higher than 450 mV. In this (still low carrier injection) regime the slope is with very high accuracy confirmed to indeed be equal to the thermal voltage (m=1).

Charge carrier lifetimes

In the following we will aim to highlight that the charge carrier lifetimes as obtained by TPV, OCVD or impedance measurements, may in fact have very little to do with steady state bulk carrier lifetimes in many studied novel thin film photovoltaic technologies.

Large signal voltage decay measurement (OCVD) is one of the earlier[4] methods to determine charge carrier recombination dynamics. **Figure 3** shows the measured 1 sun OCVD traces for the four studied solar cells (solid lines) plotted together with the calculated voltage decay of a pure geometric capacitor discharging over a cell with diode characteristics from figure 1 (dashed lines), as outlined earlier.[2, 15]

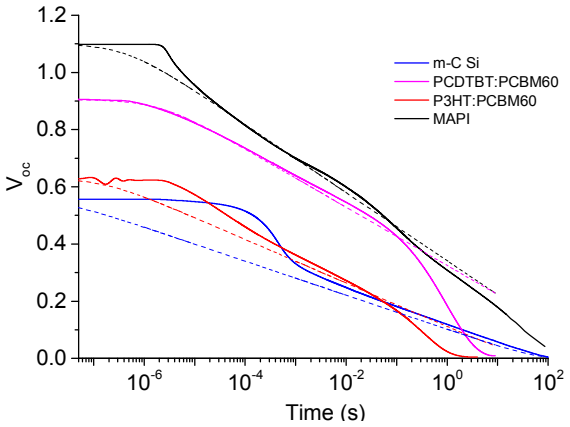

Figure 3. OCVD traces from one sun intensities for the four different studied cells. Dashed lines marks fits to a pure geometric capacitance-diode decay. In the organic cells at lower voltages the capacitive decay becomes governed by leakage current/shunts rendering a faster RC decay[2].

The first order lifetime is commonly determined from the inverse slope of OCVD according to Lederhandler[4], but only if a voltage independent slope (on linear time-axis) is observed can true first order recombination dynamics be confirmed. A pseudo-first-order lifetime as a function of the instantaneous voltage can nonetheless be calculated by the inverse differential of the OCVD trace according to[7, 40]

$$\tau_{OCVD} = -\frac{nkT}{q}\left(\frac{dV_{OC}(t)}{dt}\right)^{-1} \qquad [3]$$

View Article Online
DOI: 10.1039/C7EE03155F
ARTICLE Journal Name

where kT has its usual meaning and n is the steady state device ideality factor. Prior to taking the derivative of the OCVD signal it is necessary to employ suited smoothing functions. Here we employ logarithmic or linear LOESS smoothing in Origin as outlined in **Figure S2** in the supplementary information. The main benefit of employing the large OCVD signal instead of the small perturbation method is found in that it is a continuous measurement providing extremely high resolution in voltage and normally collected in a quite short time. Small perturbation transient photovoltage (TPV) is then performed for all devices, at an as large range as possible of background illumination intensities, and the mono-exponential lifetimes are determined. (**Figure S3** in the supplementary information provides examples of a few measured and fitted TPV traces for the studied devices.) **Figure 4** displays the obtained (pseudo-first-order) lifetimes as determined by eqn. 3 from the OCVD data together with the small perturbation TPV lifetimes obtained at logarithmically spaced steady state background illumination intensities (linear spaced open circuit voltages). We confirm that the obtained lifetimes and their relation to V_{OC} indeed are identical within very respectable accuracy for all materials apart from the perovskite cell where the slightly altering OCVD slopes[6] may not be so surprising considering the well-known influence of hysteresis, ion migration, and suggested "Tebbing" effect[19] on time resolved measurements. TPV additionally provides two clearly identifiable lifetimes in the high voltage regime of the Si cell, whereas the OCVD mainly succeeds in identifying the longer lifetime. That the inverse derivative of the large signal OCVD generally equals small perturbation lifetimes was also observed by Zaban[7] via IMVS and Barnes[40] via TPV for DSSC and Pockett[41] for perovskites (IMVS) quite recently.

Having credibly confirmed the overall identity between the OCVD and TPV lifetimes in all four devices, we can proceed by evaluating the general behavior of how this determined pseudo-first-order lifetimes relates to internal voltage. For the Hamamatsu Si photodiode, two quite constant charge carrier lifetimes are found for all voltages above ~0.4 V. These lifetimes are individually associated with the thin back p-layer and the front thicker n-layer. Accordingly, the recombination is truly of first order type in this regime of the Si photodiode, as expected. At lower voltages

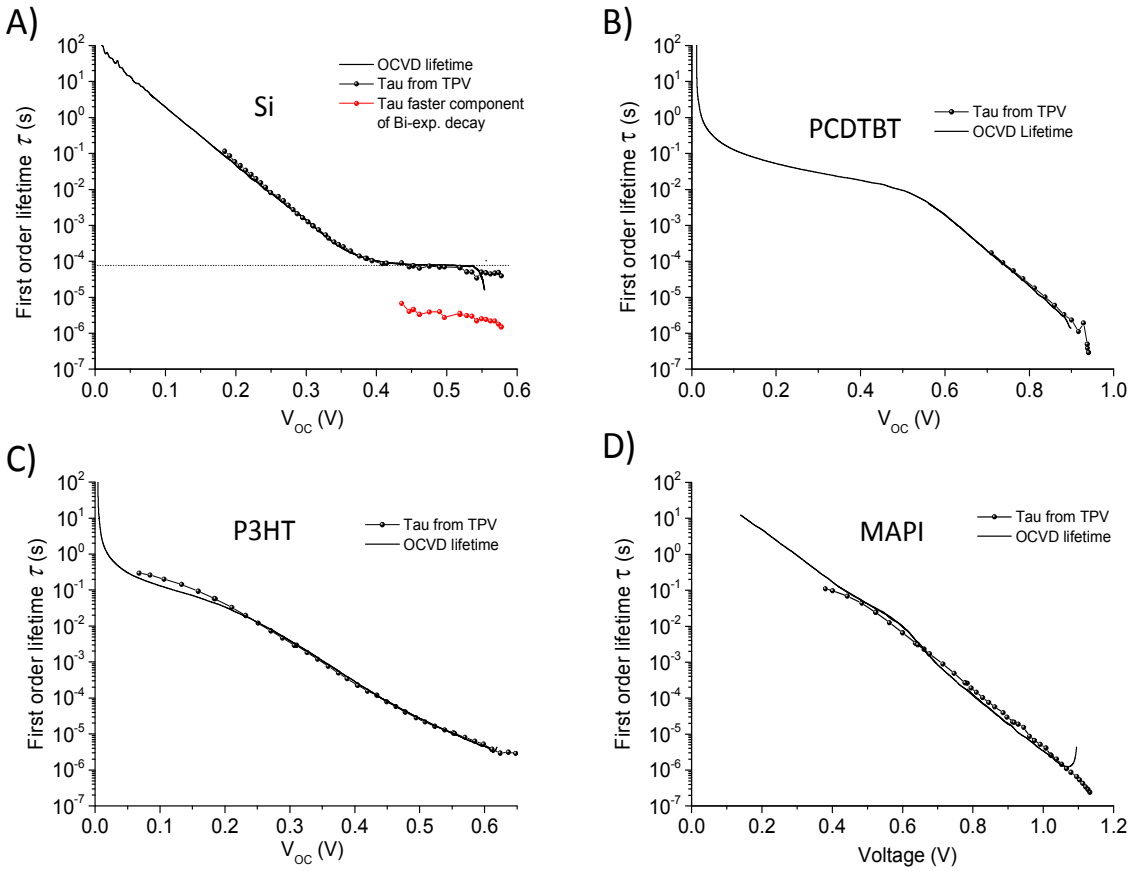

Figure 4. Lifetimes as determined via TPV and OCVD for the four cells.

View Article Online
DOI: 10.1039/C7EE03155F
Journal Name ARTICLE

only one value can however be recognized. In this regime the determined lifetime is however rapidly increasing with decreasing voltage, identically from both the TPV and OCVD measurements. Our large set of TPV illumination intensities as well as the OCVD measurements easily allows identifying that in this region the logarithm of the lifetime scales linear with voltage. This is however the regime where the determined "lifetime" has actually lost its original relevant physical meaning, as first pointed out by Mahan and Barnes.[5] Here, the measured longer "lifetime" is instead only associated to the actual discharging rate of the remaining spatially separated quasi-static capacitive charge carriers, and not at all related to the bulk recombination rate under steady state conditions. As it is impossible that the dominant recombination dynamics should make a transition from a clear first order process at high carrier densities to a higher order process at low carrier densities, this much slower low voltage decay does not represent any second or higher order recombination but instead a junction capacitive discharging rate, whose timescale is unrelated to actual bulk carrier recombination in the steady state. The PCDTBT cell does on the other hand show the strongly voltage dependent lifetime in the high voltage regime, to instead become almost constant at lower voltages. We emphasize here that in this low voltage regime the decay is however fully ruled by leakage current/shunt resistance, not present in the Si photodiode.[2] The measured slope of that regime of the OCVD trace is accordingly only a R_{shunt}-C-lifetime of the device, which indeed is quite constant. Thus, the two different regions identified in this thin film OPV device is in fact a capacitive discharging either over the material (higher voltage regime) or via the shunt path (lower voltage regime). Neither one of these regions has therefore anything to do with charge carrier lifetimes in the bulk under steady state conditions. The P3HT cell shows similar shunt decays at lower voltages as well as the voltage dependent capacitive lifetimes at intermediate voltages. However, the P3HT cell also shows a tendency of another slightly slower component starting to appear at the higher voltages. Such a deviating regime is easily identified in the Si cell, not present in the studied PCDTBT and MAPI cell, but possibly discernable for the P3HT device. Only if such a regime can be identified it is possible to also assign it to bulk relevant lifetimes. At intermediate and lower voltages none of the "lifetimes" in Figure 4 are thus related to steady state bulk carrier lifetimes. A similar lifetime concern as detailed herein via time domain methods has recently also been mentioned by Bisquert et. al. for DSSC[42], Lin et. al. for thin PbS solar cells[43] and Pocket et. al. for perovskites[41, 44] employing frequency domain methods.

View Article Online
DOI: 10.1039/C7EE03155F
ARTICLE Journal Name

Effect on the voltage decay by external conditions

To ascertain the rationality of the "lifetime" assignment we here modify external parameters that should affect the influence of junction capacitive discharging rates, but leave the bulk recombination dynamics unaffected. By first changing the starting steady state voltage by employing varying light intensities covering several decades, we show in **Figure 5** that the two OCVD regimes of the Si cell can be clearly separated, and that the attendance of the early regime is indeed intensity dependent. Although the starting (steady state) voltage scales perfectly with the logarithm of the light intensity, the initial decay is quite different depending on the starting value. The silicon cell reveals the early (relevant) decay only at intensities above 0.01 suns whereas the P3HT and MAPI device requires 1 sun to identify a slightly differing decay. At later times, all decay curves however converge to one and the same capacitive discharging trace. To further assure the capacitive assignment in these measurements, **Figure 6** displays the influence of two external components on the OCVD traces. By first placing additional capacitors (of 6.8 or 15 nF) in parallel with the solar cells under study we simply prolong the decay in a linear fashion, but only in the later capacitive region of the OCVD trace. This is the first experimental confirmation that also the pure cells are (to very different extent) here fully ruled by the relaxation of spatially separated capacitive, and not bulk, charge carriers.

To then finally ascertain that this long-lived decay is indeed only associated with carriers stored at or in the direct vicinity of the electrodes, we connect various shunt resistances in parallel with the device. These external loads evidently speed up the decay and substantially reduce the assigned "lifetimes", but again only in the time region that was ruled by the capacitive discharging. As the charges located at the electrodes are now provided with an alternative faster route to relax, a simple external resistor, their decay can indeed also be well described by a simple mono-exponential RC decay[2]. Bulk carrier recombination rates certainly remain unaffected (panel 6A) by external shunting, as expected as long as the shunt is not also limiting the

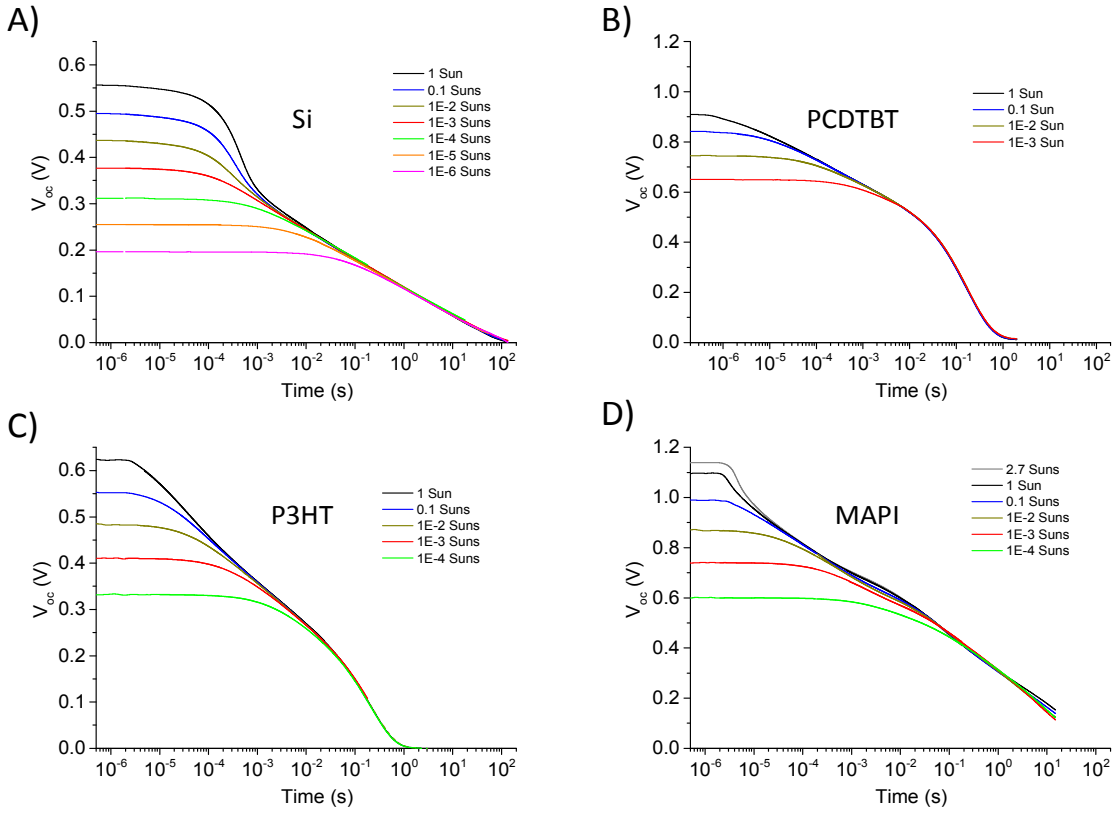

Figure 5. OCVD traces with various sets of starting voltages set by changing the light intensity.

View Article Online
DOI: 10.1039/C7EE03155F
Journal Name ARTICLE

steady state V_{OC} itself.[2] **Figure S4** in the supplementary information displays the corresponding dark I-V curves of the shunted devices. This shunting methodology is therefore very much in line with M.A. Greens suggestion of compensated OCVD measurements[45] which allows reducing the influence of the capacitive charges on the measurements. This is accordingly the second strong confirmation that the decay at intermediate voltages, where the lifetime scales clearly exponentially with voltage, is indeed only associated with carriers located at the electrodes and not necessarily with carriers trapped in tail states of the DOS in the bulk of the material. Such carriers can only be released thermally or by applying an external electric field but would not notice whether the electrodes are shunted or not.

For the PCDTBT cell we again confirm that the entire time regime was ruled exclusively by such a geometric capacitive decay. For the MAPI cell we propose that the initial quite constant voltage of the OCVD trace is most likely an effect originating from some form of ionic capacitance, as noted earlier for perovskites.[6, 44] We indeed see that the OCVD lifetime and TPV lifetime are actually differing somewhat at the highest voltages for the MAPI cell (figure 4D). As TPV better represents steady state conditions we prefer to here put more trust in the high voltage TPV lifetime measurements, which also do not show any clear deviation from the behavior at the intermediate voltages. The remaining question is then what the early slightly slower decay should be assigned to in the P3HT cell. One of our main proposals here is that only if such a distinguishable slower decay component can be identified at higher voltages and early timescales, one that also vanishes at the lower voltages in the capacitive decay regime, is it *possible* to assign it to real steady state bulk related recombination kinetics, but unfortunately still not necessarily so, as also

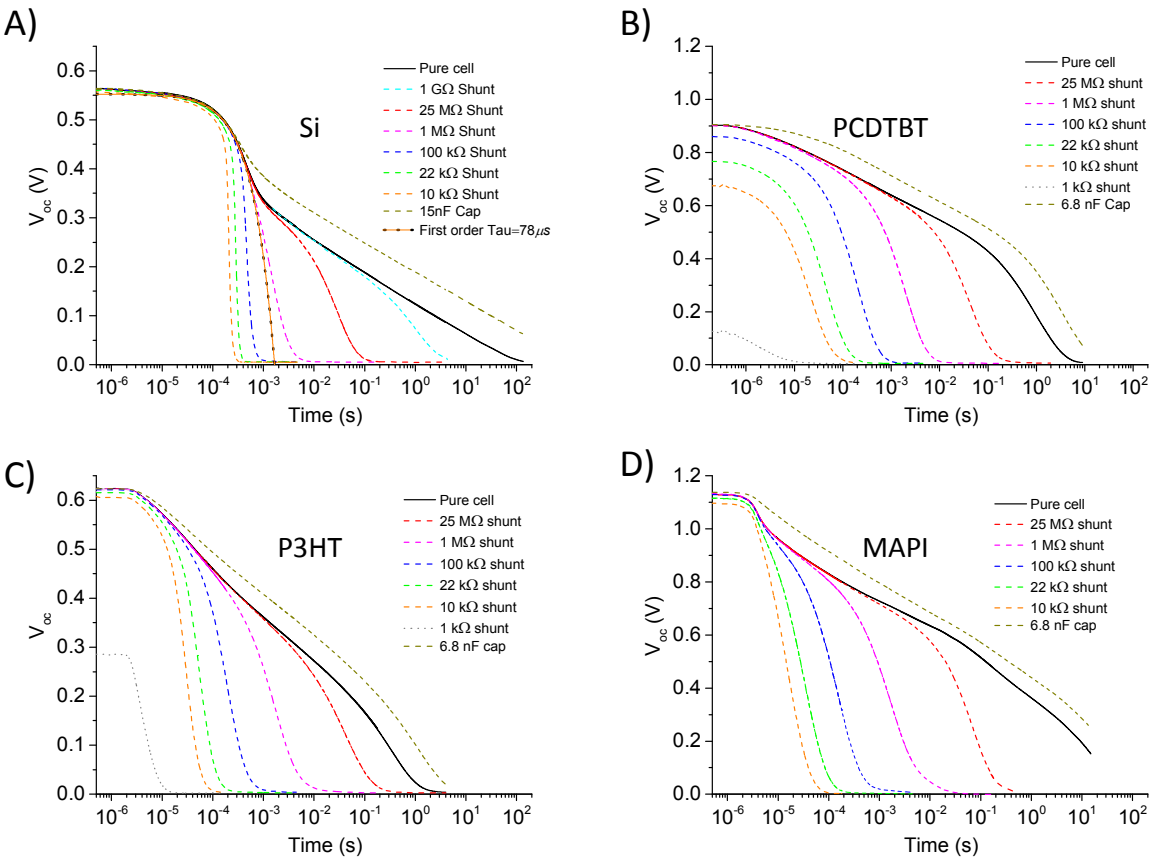

Figure 6. OCVD with external capacitors and shunt resistors. The voltage decay associated with capacitive charges is prolonged with an additional capacitor in parallel, but only in the time region where the device capacitance is the main contributor to the decay. At timescales earlier than 1ms for the Si cell the additional capacitance have no influence, as the bulk charges are here still outnumbering the capacitive ones, and the total decay is thus ruled by their recombination rate. For the PCDTBT cell we note on the other hand that the extra capacitance is affecting the entire voltage decay. By instead placing shunts in parallel with the devices we open up a new quicker (at lower voltages) decaying route for the capacitive charges located at the electrode.

View Article Online
DOI: 10.1039/C7EE03155F

voltage dependent capacitance may still play a role here. For the P3HT cell we are also aware of that the C-V measurements does show a voltage dependence that cannot accurately be described by an abrupt depletion layer approximation according to Mott-Schottky, but instead by a power law behavior more similar to those of hyper-abrupt junctions[46] and with a built-in-potential very close to the actual open circuit voltage around 1 sun. The initial decay of such devices may thus still be affected by capacitive effects that are not necessarily associated with a constant capacitance discharging over a diode as the dashed lines in Figure 3 represents.

Analytical limit for lifetime derived from the Si cell capacitive decay.

To narrow down the regions of useful lifetime information available in electrical transient measurements of solar cells, we in this section re-evaluate the analytical approach for charge control in a diode as proposed by Castaner.[47, 48] The two clear processes identified in the Si photodiode allows for a quite simple analytical expression of the entire voltage decay of the device. The differential equation for charge control ($Q(t)$) in a diode with the inclusion of an arbitrary form of capacitance (internal or external) operating in the low injection regime reads:

$$\frac{dQ(t)}{dt} = -\frac{Q(t)}{\tau_{Bulk}} - C\frac{dV(t)}{dt} \qquad [4]$$

where τ_{Bulk} is a real first order lifetime of excess minority carriers and C is the device capacitance (which may also be voltage dependent if e.g. a depletion layer approximation is instead suited). Note that we in eqn. 4 are for clarity omitting any high injection regime second or higher order recombination, as we know that these are not present in this device at the evaluated intensities. The second capacitive term has in a many earlier rate equations for thin film PVs unfortunately not been accounted for, but is very necessary if the sample has electrodes present. Analytical solution to eqn. 4 exists and is provided already by Castaner[47, 48] for $t(V_{OC})$ if one assumes a constant geometric capacitance, which to a first approximation is sufficient for our here intended message. **Figure 7A** shows the analytical solution to eqn. 4 with unity ideality factor and constant capacitance being a factor two higher than the measured geometric and by Hamamatsu stated capacitance. The Si cell does however show a clear depletion layer capacitance, for which numerical solutions to eqn. 4 are instead necessary, but for clarity we choose to follow the analytical solution by Castaner employing a constant, but slightly higher than the measured geometric capacitance. From this relationship, we can then directly calculate the pseudo-first order analytical lifetimes via eqn. 3 which is plotted in **Figure 7B** together with *measured* pseudo-first order lifetimes for the Si photodiode. The inset equation in Figure 7B is obtained via eqn. 3 using the chain rule and provides the determined lifetime as a function of open circuit voltage. The influence of the different contributions to "*lifetimes*" becomes very obvious and the analytical expression clearly shows when the relevant steady state bulk carrier lifetime is measurable, depending on the values in the second term

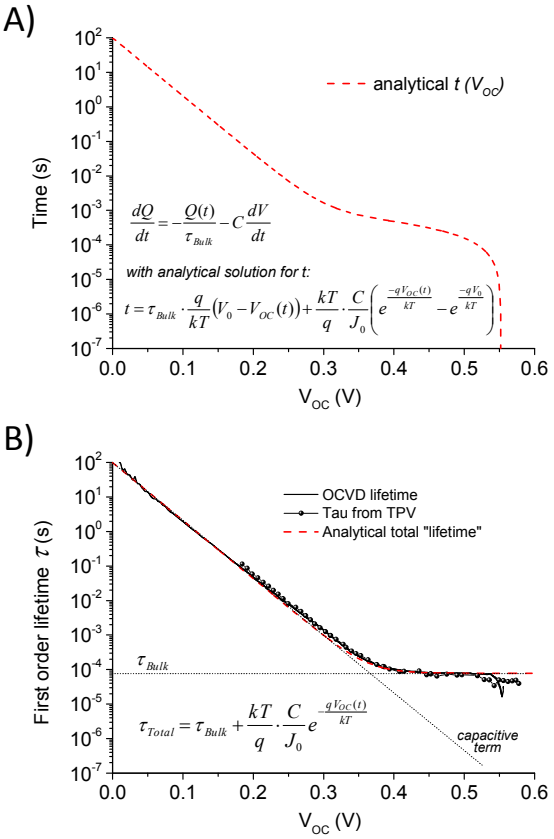

Figure 7. A) Analytical solution to eqn. 4 accounting for a real first order lifetime and the contribution from capacitive relaxation. B) Corresponding calculated pseudo-first order "lifetime" together with measured ones from OCVD and TPV. The dark saturation current of 52 nA/m^2 used in the analytical expression is obtained from the dark I-V presented in figure 1 and the capacitance value used is an effective approximation of the true depletion layer capacitance which amounted here to 2E-4 F/m^2 (a factor of two higher than the true geometric capacitance).

View Article Online
DOI: 10.1039/C7EE03155F
Journal Name ARTICLE

of the right hand side of the equation. This "capacitance-diode" term is obviously exponentially dependent on the instantaneous value of the voltage itself. Accordingly, for an accurate assignment of true steady state bulk related carrier lifetimes via transient electrical measurements, the following relation must always hold:

$$\tau_{Bulk} >> \frac{nkT}{q}\cdot\frac{C}{J_0}\cdot e^{-\frac{qV_{OC}}{nkT}} = \frac{CnkT}{q\cdot J_{SC}(V_{OC})} \qquad [5]$$

independent if it is a true first order constant lifetime or higher order density dependent "lifetimes". Herein we have now also included the diode ideality factor and identified the total recombination current[36] at V_{OC} as equal the short circuit current ($J_{REC}(V_{OC})=J_{SC}$). All parameters of eqn. 5 are hence experimentally directly accessible. The relationship between J_{SC} and V_{OC} is therefore provided in the supplementary information (**Figure S5)** together with the corresponding dark J-Vs of all devices. eqn. 5 thus embodies the main message of this contribution. Only if eqn. 5 holds can one actually use electrical means to determine bulk carrier lifetimes relevant under steady state conditions. From a strict experimental lifetime determination point of view, it becomes clear that two things should always be strived for: large recombination currents i.e. higher voltages (stronger illumination) and low capacitances (thicker devices). The main limitation of lifetime determination via electrical means arises accordingly from the fact that the relaxation of charges associated with the quasi-static capacitance of geometrical or space-charge regions in the device is also a negative exponential function of the open circuit voltage, just like the earlier assumed empirical relation of eqn. 1. With a depletion layer capacitance instead of the above assumed geometric capacitance, the small voltage dependence of C in eqn. 5 will alter the minimum lifetime slightly, but the overall equation with constant geometric capacitance suffices as an analytically derivable and still very useful rule.[47] Our here used high quality Si photodiode has a sufficiently long lifetime to easily pass the test of eqn. 5 as long as we are evaluating light intensities higher than 0.01 suns, whereas the other cells are more questionable. To further highlight the influences of light intensity and capacitance on the decaying voltage we illustrate in **Figure S6** in the supplementary information some direct analytical outcomes of eqn. 4.

We emphasize that the expression for the capacitance discharging lifetime is in form quite identical to that obtained (eqn. 1) when assuming exclusive higher order recombination,[8, 9, 29, 49] apart from that the prefactor (τ_0 in those earlier expressions) is now well defined and ruled by ratio between the capacitance and the dark saturation current of the cell, and not at all equal to thermal equilibrium lifetimes. The unit remains time, but the fact that it is ruled by the capacitance explains the extremely high value it so often needed to take in earlier literature. We also note that the denominator in the exponent of our here stated geometric limit is *nkT* but would be slightly larger if a voltage dependent capacitance is instead existing, and fitted with a pure exponential function as that in eqn.1 with the denominator being *vkT*. Accordingly, irrespective of the real bulk lifetime is a true first order (carrier density independent) lifetime or a second or higher order density dependent "lifetime" its value specified at any voltage *must always be much larger* than the right-hand side of eqn. 5. **Figure 8** finally plots the outcome of this calculated minimum lifetime from eqn. 5 vs. the measured lifetime from the OCVD (and TPV) method. The geometric capacitance values are determined via low frequency C-V measurements (Figure S1). As the Si diode showed clear depletion layer capacitance we have for this device included both the analytical limit from the stated geometric capacitance (blue dashed) as well as the limit originating from a Mott-Schottky analysis and numerical solution to eqn. 4 (green dashed).

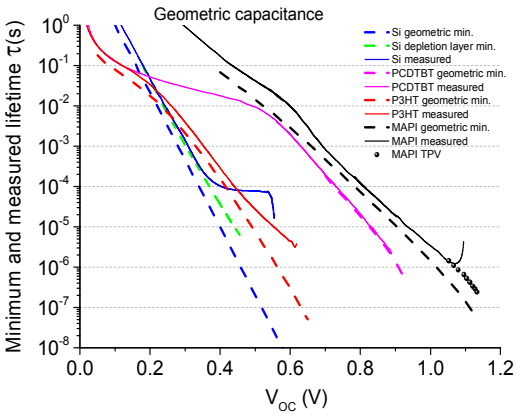

Figure 8. Electrical limit for lifetimes vs. the measured lifetimes. Dashed lines are minimum lifetimes as determined via eqn. 5 employing the geometric constant capacitance. Green dashed line also shows the example of the depletion layer capacitance limit for the Si cell, shifting the limit on top of the measured lifetime in the low voltage range. We propose that other forms of (non-geometric type) capacitances explain the remaining small offset for the MAPI (ion redistribution) and P3HT (hyper abrupt junction).

View Article Online
DOI: 10.1039/C7EE03155F

As clearly can be seen in Figure 8, it is only the Si photodiode that certainly passes the constraint of eqn. 5 for measured lifetimes above 450 mV. The PCDTBT is not safe in any region and every assigned "lifetime" is, as stated earlier, a full geometric capacitive decay. For the P3HT cell we can identify a departure from the geometric capacitive lifetime at the highest voltages, yet its departure is not large enough to not still be partly affected. For this device, we also note that the capacitance itself does show a pronounced voltage dependence, yet not possible to fit with the simple Mott-Schottky expression. Such additional junction capacitive effects are also likely the reason for that a small offset remains (approximately a factor of 2) between the calculated geometric minimum lifetime and the measured one for both the P3HT and the MAPI cells.

We conclude this part by proposing the obvious; provided that measured lifetimes as well as the parameters in eqn. 5 are all obtainable within very high accuracy over all voltages, including the true voltage dependence of a possible junction capacitance, it should be conceivable to subtract the capacitive contribution from the measured lifetime to obtain a more realistic representation of the accuracy of the electrical lifetime assignments (quite noisy, but more accurate). Thus, just as carrier densities need to be corrected for capacitance, the measured lifetimes necessarily need to be accurately corrected for the capacitive decay!

Conclusion

This work proposes a resolution to the now long-standing controversy of reported charge carrier lifetimes often observed in thin film photovoltaic devices such as OPVs, PbS, DSSC, as well as in perovskite solar cells. We provide clear evidence that the voltage decay of these cells are mostly governed by capacitive electrode associated charges that makes bulk carrier lifetime assignments relevant under steady state conditions very difficult. These spatially separated charges are located either close to the charge selective layers, in the charge selective layers, or in the actual conducting metal electrodes. We have herein refrained from pinpointing their exact location and spatial distribution, but leave that to carrier density simulation methods such as *transient* drift diffusion modelling, but clearly state that these long lived carriers are not allocated in the bulk of the absorbing semiconductor. The problem of relevant lifetime determination via electrical means arises solely from that the relaxation of charges associated with a quasi-static capacitance of geometric or space-charge regions in the device is always a decaying exponential function of the instantaneous open circuit voltage, as outlined in eqn. 5. If the restrictions of this equation do not hold, one is unquestionably measuring mostly capacitive discharging rates as well as charge "densities" stored in or at the surfaces of the device, as opposed to in the sought-after bulk region. We therefore state that only if the relevant steady state decay rate of bulk charge carriers is substantially slower than the decay rate of capacitive space charges can it be safely measured via electrical transient means. We also note that these concerns were long ago identified within the field of older inorganic *p-n* PV technologies, where electrical lifetime measurements were initially conducted.[5, 45, 50] Even if carrier densities have previously been partly corrected for capacitance in most novel thin film solar cells, the discharging rate and redistribution of these (still present) carriers have not been adequately accounted for in lifetime assignments. Considering the vast literature in OPVs, PbS, DSSC and perovskite PV, that are all observing higher order recombination in combination with overall very slow recombination rates, we believe the much simpler description presented herein is in many cases more probable.

Conflicts of interest

There are no conflicts to declare.

Acknowledgements

K.T acknowledges the German Research Foundation (DFG) for funding through project 382633022 (RECOLPER). The work was further supported by the German Federal Ministry for Education and Research (BMBF) through the grant 03SF0514 (HYPER).

K.T. and A.B. designed study which D.K., KT. and M.F. implemented experimentally. D.K. measured TPV and CE, M.F. measured C-V. D.K. and K.T. measured OCVD, I-V and $J_{SC}(V_{OC})$. K.T and D.K. analyzed the data. K.T. wrote the paper. All authors contributed with discussion, feedback and comments to the manuscript.

View Article Online
DOI: 10.1039/C7EE03155F
Journal Name ARTICLE

Notes and references

1. S. De, T. Pascher, M. Maiti, K. G. Jespersen, T. Kesti, F. L. Zhang, O. Inganas, A. Yartsev and V. Sundstrom, *J Am Chem Soc*, 2007, **129**, 8466-8472.
2. K. Tvingstedt, L. Gil-Escrig, C. Momblona, P. Rieder, D. Kiermasch, M. Sessolo, A. Baumann, H. J. Bolink and V. Dyakonov, *Acs Energy Lett*, 2017, **2**, 424-430.
3. K. Tvingstedt, O. Malinkiewicz, A. Baumann, C. Deibel, H. J. Snaith, V. Dyakonov and H. J. Bolink, *Sci Rep*, 2014, **4**, 6071.
4. S. R. Lederhandler and L. J. Giacoletto, *Proc Ire*, 1955, **43**, 477-483.
5. J. E. Mahan and D. L. Barnes, *Solid State Electron*, 1981, **24**, 989-994.
6. A. Baumann, K. Tvingstedt, M. C. Heiber, S. Vath, C. Momblona, H. J. Bolink and V. Dyakonov, *Apl Mater*, 2014, **2**, 081501.
7. A. Zaban, M. Greenshtein and J. Bisquert, *Chemphyschem*, 2003, **4**, 859-864.
8. C. G. Shuttle, B. O'Regan, A. M. Ballantyne, J. Nelson, D. D. C. Bradley, J. de Mello and J. R. Durrant, *Appl Phys Lett*, 2008, **92**, 093311.
9. A. Maurano, C. C. Shuttle, R. Hamilton, A. M. Ballantyne, J. Nelson, W. M. Zhang, M. Heeney and J. R. Durrant, *J Phys Chem C*, 2011, **115**, 5947-5957.
10. T. M. Clarke, C. Lungenschmied, J. Peet, N. Drolet and A. J. Mozer, *Adv Energy Mater*, 2015, **5**, 1401345.
11. L. Bertoluzzi, P. P. Boix, I. Mora-Sero and J. Bisquert, *J Phys Chem C*, 2014, **118**, 16574-16580.
12. I. Mora-Sero, G. A. Garcia-Belmonte, P. P. Boix, M. A. Vazquez and J. Bisquert, *Energ Environ Sci*, 2009, **2**, 678-686.
13. V. V. Brus, C. M. Proctor, N. A. Ran and T. Q. Nguyen, *Adv Energy Mater*, 2016, **6**, 1502250.
14. P. R. F. Barnes, A. Y. Anderson, M. Juozapavicius, L. X. Liu, X. E. Li, E. Palomares, A. Forneli and B. C. O'Regan, *Phys Chem Chem Phys*, 2011, **13**, 3547-3558.
15. E. H. Hellen, *Am J Phys*, 2003, **71**, 797-800.
16. N. W. Duffy, L. M. Peter, R. M. G. Rajapakse and K. G. U. Wijayantha, *J Phys Chem B*, 2000, **104**, 8916-8919.
17. B. C. O'Regan and F. Lenzmann, *J Phys Chem B*, 2004, **108**, 4342-4350.
18. V. Roiati, S. Colella, G. Lerario, L. De Marco, A. Rizzo, A. Listorti and G. Gigli, *Energ Environ Sci*, 2014, **7**, 1889-1894.
19. B. C. O'Regan, P. R. F. Barnes, X. E. Li, C. Law, E. Paomares and J. M. Marin-Beloqui, *J Am Chem Soc*, 2015, **137**, 5087-5099.
20. G. S. Han, H. S. Chung, B. J. Kim, D. H. Kim, J. W. Lee, B. S. Swain, K. Mahmood, J. S. Yoo, N. G. Park, J. H. Lee and H. S. Jung, *J Mater Chem A*, 2015, **3**, 9160-9164.
21. Y. C. Shao, Y. B. Yuan and J. S. Huang, *Nature Energy*, 2016, **1**, 15001.
22. J. P. Correa-Baena, W. Tress, K. Domanski, E. H. Anaraki, S. H. Turren-Cruz, B. Roose, P. P. Boix, M. Gratzel, M. Saliba, A. Abate and A. Hagfeldt, *Energ Environ Sci*, 2017, **10**, 1207-1212.
23. C. Tao, J. Van der Velden, L. Cabau, N. F. Montcada, S. Neutzner, A. R. S. Kandada, S. Marras, L. Brambilla, M. Tommasini, W. D. Xu, R. Sorrentino, A. Perinot, M. Caironi, C. Bertarelli, E. Palomares and A. Petrozza, *Adv Mater*, 2017, **29**, 1604493.
24. J. M. Marin-Beloqui, L. Lanzetta and E. Palomares, *Chem Mater*, 2016, **28**, 207-213.
25. D. Kiermasch, P. Rieder, K. Tvingstedt, A. Baumann and V. Dyakonov, *Sci Rep*, 2016, **6**, 39333.
26. E. Guillen, F. J. Ramos, J. A. Anta and S. Ahmad, *J Phys Chem C*, 2014, **118**, 22913-22922.
27. C. Vanberkel, M. J. Powell, A. R. Franklin and I. D. French, *J Appl Phys*, 1993, **73**, 5264-5268.
28. S. A. Hawks, G. Li, Y. Yang and R. A. Street, *J Appl Phys*, 2014, **116**, 074503.
29. T. Kirchartz and J. Nelson, *Phys Rev B*, 2012, **86**, 165201.
30. F. Etzold, I. A. Howard, R. Mauer, M. Meister, T. D. Kim, K. S. Lee, N. S. Baek and F. Laquai, *J Am Chem Soc*, 2011, **133**, 9469-9479.
31. D. Jarzab, F. Cordella, J. Gao, M. Scharber, H. J. Egelhaaf and M. A. Loi, *Adv Energy Mater*, 2011, **1**, 604-609.
32. D. Veldman, O. Ipek, S. C. J. Meskers, J. Sweelssen, M. M. Koetse, S. C. Veenstra, J. M. Kroon, S. S. van Bavel, J. Loos and R. A. J. Janssen, *J Am Chem Soc*, 2008, **130**, 7721-7735.
33. B. Bernardo, D. Cheyns, B. Verreet, R. D. Schaller, B. P. Rand and N. C. Giebink, *Nat Commun*, 2014, **5**, 3245.
34. F. Deledalle, P. S. Tuladhar, J. Nelson, J. R. Durrant and T. Kirchartz, *J Phys Chem C*, 2014, **118**, 8837-8842.
35. F. Deledalle, T. Kirchartz, M. S. Vezie, M. Campoy-Quiles, P. S. Tuladhar, J. Nelson and J. R. Durrant, *Phys Rev X*, 2015, **5**, 0111032.
36. K. Tvingstedt and C. Deibel, *Adv Energy Mater*, 2016, **6**, 1502230.
37. R. A. Sinton and A. Cuevas, *Appl Phys Lett*, 1996, **69**, 2510-2512.
38. C. Deibel, A. Wagenpfahl and V. Dyakonov, *Phys Rev B*, 2009, **80**, 075203.
39. I. Zonno, A. Martinez-Otero, J. C. Hebig and T. Kirchartz, *Phys Rev Appl*, 2017, **7**, 034018.
40. P. R. F. Barnes, K. Miettunen, X. E. Li, A. Y. Anderson, T. Bessho, M. Gratzel and B. C. O'Regan, *Adv Mater*, 2013, **25**, 1881-1922.

View Article Online
DOI: 10.1039/C7EE03155F

41. A. Pockett, G. E. Eperon, T. Peltola, H. J. Snaith, A. Walker, L. M. Peter and P. J. Cameron, *J Phys Chem C*, 2015, **119**, 3456-3465.
42. J. Bisquert, F. Fabregat-Santiago, I. Mora-Sero, G. Garcia-Belmonte and S. Gimenez, *J Phys Chem C*, 2009, **113**, 17278-17290.
43. W. M. M. Lin, D. Bozyigit, O. Yarema and V. Wood, *J Phys Chem C*, 2016, **120**, 12900-12908.
44. A. Pockett, G. E. Eperon, N. Sakai, H. J. Snaith, L. M. Peter and P. J. Cameron, *Phys Chem Chem Phys*, 2017, **19**, 5959-5970.
45. M. A. Green, *Solid State Electron*, 1983, **26**, 1117-1122.
46. M. H. Norwood, *Proc Inst Electr Elect*, 1968, **56**, 788.
47. L. Castaner, E. Vilamajo, J. Llaberia and J. Garrido, *J Phys D Appl Phys*, 1981, **14**, 1867-1876.
48. L. Castaner and J. Cabestany, *Proc 1st Europ. Symp. Photovoltaic Generators in Space*, 1978, **1**.
49. A. Foertig, J. Rauh, V. Dyakonov and C. Deibel, *Phys Rev B*, 2012, **86**, 115302.
50. J. J. Liou and F. A. Lindholm, *Solid State Electron*, 1987, **30**, 457-462

View Article Online
DOI: 10.1039/C7EE03155F

Journal Name

ARTICLE